# scientific reports

OPEN

# Modulation of consciousness in disorders of consciousness by HD-tDCS targeting frontal and posterior cortical regions

Yongkun Guo[1,3,6], Yuan Zhong[2,6], Anqin Dong[1], Wanqing Liu[1], Shuai Han[5], Kang Zhang[4], Jingwei Xie[1], Pengyuan Zheng[1], Yihua Wang[2✉] & Chunyun Zhang[2✉]

The search for neural correlates of consciousness has always been a hot topic in the field of consciousness. Previous studies have shown that high-density transcranial direct current stimulation (HD-tDCS) can promote the recovery of consciousness level in patients with disorders of consciousness (DOC). This study intends to explore the neuromodulatory effects of HD-tDCS at different target from the perspectives of brain spatiotemporal dynamics and directed information flow, thereby clarifying the key brain areas for the origin of consciousness. The study prospectively used a high-density transcranial direct current stimulation (HD-tDCS) protocol to perform repeated stimulation at different target points for 46 DOC patients (F3 group, $n = 11$; sham group, $n = 19$; Pz group, $n = 16$). The Coma Recovery Scale-Revised (CRS-R) index was calculated, and microstate analysis and symbolic transfer entropy(STE) brain network construction were performed before and 14 days after HD-tDCS stimulation. We identified seven microstates with different spatial distributions of electrode activation. There were significant differences in microstates (including spatial activation patterns and brain dynamics) for different stimulation protocols. At the same time, the F3 group strengthened the information flow from the anterior to the posterior brain and internal information flow in the anterior brain in the theta band, while the Pz group mainly increased the information flow between the left frontal and parietal lobes in the theta and alpha bands. The study suggests that consciousness is the result of the comprehensive action of the anterior and posterior brain, and there is an overlap in the mechanisms of action between the two HD-tDCS stimulation protocols, suggesting that a multi-target combined stimulation protocol may be a potentially better stimulation scheme.

**Keywords** Disorders of consciousness, Microstate, Symbolic transfer entropy, Transcranial direct current stimulation

The scientific study of consciousness has been primarily focused on identifying the 'neural correlates of consciousness' (NCC). In formal terms, the NCC of a conscious state constitute the minimal neural events that are jointly sufficient to produce that conscious experience. In practice, the quest for NCC has been about identifying brain states and processes most intimately connected with consciousness. A plethora of candidate theories of consciousness (ToCs) have emerged. Notably, none of these theories pinpoint a specific region within the brain as the exclusive birthplace of consciousness. Current consciousness theories include, among others, the higher-order thought theory (HOTs), the global workspace theory (GWTs), the integrated information theory (IIT), and the reentry and predictive processing theory (PP), each offering distinct perspectives on the origins and nature of consciousness[1]. The HOTs posits that a conscious state becomes conscious because it is the target of a specific type of meta-representation[2]. The GWTs suggests that conscious experiences arise from the global accessibility of information across the brain, typically involving networks associated with the frontal and parietal lobes[3,4]. The IIT proposes that consciousness is associated with the causal structure of irreducible integrated

[1]Department of Neurosurgery, Fifth Affiliated Hospital of Zhengzhou University, Zhengzhou 450000, China. [2]Department of Neurosurgery, Qilu Hospital of Shandong University(Qingdao), Qingdao 266000, China. [3]Henan Engineering Research Center for Prevention and Treatment of Brain Injury, Zhengzhou 450000, China. [4]Department of Neurosurgery, First Hospital of Jilin University, Changchun 130021, China. [5]Department of Neurosurgery, Beijing Tiantan Hospital, Capital Medical University, Beijing, China. [6]Yongkun Guo and Yuan Zhong contributed equally to this work. ✉email: wyh120071@qlyyqd.com; Chunyun_Zhang@hotmail.com

information within a physical system, and is linked to certain areas in the posterior part of the brain, such as the parietal, temporal, and occipital lobes[5,6]. The PP emphasizes the role of top-down signaling within the brain in shaping conscious perception. These discussions indicate that the origin and essence of consciousness is a broad and complex issue[7].

Disorders of consciousness (DoC) result from either direct damage to the neural structures governing arousal and consciousness or indirect disruption of their connectivity. Such disorders encompass coma, characterized by a state of unconsciousness with only reflexive behaviors, the unresponsive wakefulness syndrome (UWS; previously referred to as the vegetative state, which presents with wakefulness but limited to reflexive behaviors), and the minimally conscious state (MCS), where there is clinical evidence of minimal signs of consciousness. When a patient with a disorder of consciousness (DoC) regains the ability to communicate functionally or manipulate objects, they are said to have emerged from the minimally conscious state (eMCS)[8]. The Coma Recovery Scale-Revised (CRS-R) is a reliable and sensitive clinical instrument used to differentiate between patients in UWS, MCS, and eMCS. However, this scale's assignment of consciousness levels based on the highest diagnostic score across its subscales is less suitable for tracking changes in the level of consciousness in DoC[9,10].

Anodal transcranial direct current stimulation (tDCS) is a non-invasive neuromodulation technique that increases neuronal excitability by depolarizing the resting potential[11-13]. The left dorsolateral prefrontal cortex (DLPFC) has always been a hot topic for the selection of tDCS stimulation targets. Some researchers believe that the recovery of consciousness is related to the frontoparietal network. The DLPFC is one of the main brain areas of the frontoparietal network, and once activated, it may have the capacity to transmit excitability throughout the entire cerebral cortex. Some past studies have demonstrated that tDCS can also serve as a therapeutic method, enhancing the level of consciousness in patients with DOC by stimulating DLPFC[14,15]. However, in some studies, no significant therapeutic effects were observed. Wu et al. have shown that in DOC patients, the intrinsic functional connectivity strength of many brain regions, especially in the posterior cingulate cortex and precuneus, is significantly correlated with the level of consciousness and the outcome of recovery[16]. At the same time, it is also a component of the frontoparietal network, thus the posterior cortex may serve as a potential stimulation target[17,18]. Our initial findings demonstrate that targeting the Pz region promotes consciousness recovery in patients with disorders of consciousness[19]. For DLPFC engagement, stimulation is typically administered at the F3 site, while the Pz electrode serves as the optimal target for accessing parieto-occipital lobe given its anatomical proximity. It is still unclear how tDCS acts on the functional connectivity between different brain regions and brain networks. Traditional tDCS includes two independent electrode pads, an anode and a cathode. The normal size of each electrode is about $5 \times 7$ cm. Due to its shape and the diffuse brain current, it is difficult to pinpoint the actual cortical area stimulated by tDCS. To overcome this disadvantage, researchers have modified the traditional tDCS, namely high-definition tDCS (HD-tDCS), equipped with a central anode and four surrounding cathode electrodes. Due to its small size, it has the advantage of precise spatial localization[19].

Microstate analysis offers insights into brain states, their rapid transitions during cognitive processes, and in neurological disorders. The exceptional temporal resolution of electroencephalography (EEG) renders it ideal for examining the brain's resting state and its responsiveness to stimulation. On EEG recordings, distinct topographic configurations, known as 'microstates,' remain stable for only 10–100 milliseconds before transitioning swiftly to other configurations. These microstates, often described as the "atoms of thought," are thought to encapsulate the fundamental dynamics of brain activity, oscillating rapidly between activation and deactivation in a resting state[20-22]. Observations indicate that microstate alterations occur during developmental and aging processes, as well as in a spectrum of neurological conditions such as schizophrenia, depression, and frontotemporal dementia. Consequently, EEG microstates may offer a novel lens through which to view the operation of DoC patients' brains at the millisecond level. When compared to power spectrum analysis or static functional network analysis, EEG microstates emerge as a potentially more suitable biomarker due to their superior temporal resolution[23].

Emerging methods for evaluating effective connectivity (EC) elucidate the directional flow of information across brain regions, offering deeper insights into brain networks[24,25]. Transfer entropy (TE) stands out as a particularly promising approach for assessing EC due to its model-free nature, meaning it does not rely on preconceived assumptions regarding data generation. Importantly, TE is capable of detecting nonlinear interactions within brain functions, even amidst significant interaction delays caused by the traversal of signals through multiple pathways. Of the various techniques for measuring TE, symbolic transfer entropy (STE) is distinguished by its robustness and rapid computational speed, making it an invaluable tool for analyzing information transfer within complex temporal sequences, such as those found in EEG signals[26]. EEG frequencies correlate with distinct neural activities; lower frequencies typically indicate deep sleep states, whereas higher frequencies are often linked to brain arousal or awakening. In our research, we employed STE to examine EC within these EEG frequency bands, providing a method that is not only convenient and robust but also computationally efficient for investigating information flow in dynamic, multidimensional systems, and pinpointing the principal direction of inter-regional brain information transfer.

This study investigates the arousal effects of HD-tDCS on patients with disorders of consciousness (DoC) by analyzing EEG microstates and directed functional connectivity. The research aims to elucidate the spatiotemporal dynamics of the brain and the patterns of information flow, ultimately contributing to the identification of critical brain regions associated with the emergence of consciousness. These findings are intended to augment current theories on the genesis and restoration of consciousness.

## Materials and methods
### Patients and diagnosis
Between September 2020 and October 2023, 52 patients with DoC were enlisted from the Department of Neurosurgery at the Fifth Affiliated Hospital of Zhengzhou University. Experienced clinicians utilized the CRS-R
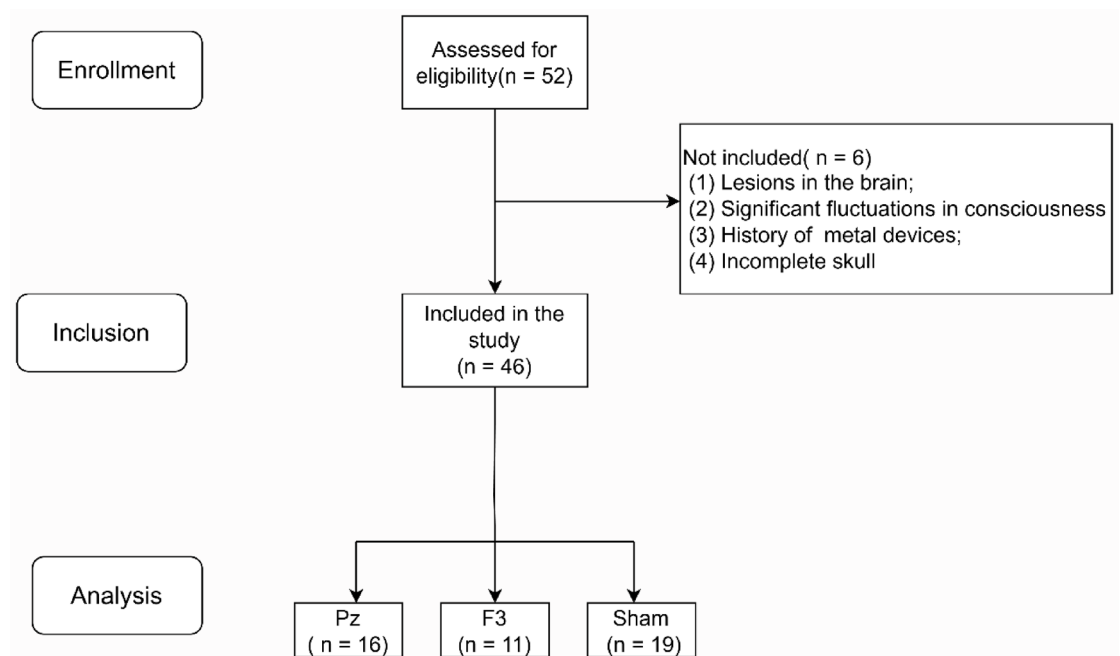
**Fig. 1**. Flowchart of study screening.

| | ALL | F3 | Sham | Pz | |
|---|---|---|---|---|---|
| | *N* = 46 | *N* = 11 | *N* = 19 | *N* = 16 | *p* |
| Gender | | | | | 0.241 |
| F* | 16 (34.8%) | 5 (45.5%) | 8 (42.1%) | 3 (18.8%) | |
| M* | 30 (65.2%) | 6 (54.5%) | 11 (57.9%) | 13 (81.2%) | |
| Age+ | 54.1 (13.7) | 55.9 (19.5) | 56.3 (7.18) | 50.3 (14.8) | 0.391 |
| Etiology | | | | | 0.583 |
| Anoxia* | 2 (4.35%) | 0 (0.00%) | 0 (0.00%) | 2 (12.5%) | |
| Stroke* | 33 (71.7%) | 8 (72.7%) | 14 (73.7%) | 11 (68.8%) | |
| TBI* | 11 (23.9%) | 3 (27.3%) | 5 (26.3%) | 3 (18.8%) | |
| T0_index+ | 16.6 (16.3) | 17.6 (19.7) | 19.2 (17.5) | 12.9 (12.3) | 0.520 |

**Table 1**. Summary of patients' characteristics by 'Target'. TBI, traumatic brain injury. * n (%) + mean (standard deviation).

to determine the CRS-R index, applying arousal stimulation protocols as needed to ascertain the patients' level of consciousness. Inclusion criteria for patients: (1) No scalp lesions or intracranial metal implants; (2) No history of neurological or psychiatric disorders; (3) No acute or chronic disease episodes; (4) Loss of consciousness for more than 28 days. The enrolled patients were divided into three groups: F3 target group, Pz target group, and sham group. Exclusion criteria included: (1) Lesions in the frontal and occipital lobes of the brain; (2) Significant fluctuations in the level of consciousness in the week before HD-tDCS stimulation; (3) History of cardiac pacemakers, aneurysm clips, or other metal devices; (4) Incomplete skull. A total of 46 patients completed the tDCS treatment, divided into the F3 target group, Pz target group, and sham group. The flowchart depicting the study process is shown in Fig. 1. The epidemiological characteristics of patients can be seen in Table 1.

The study design and implementation adhered to the principles of the Declaration of Helsinki and legally authorized representatives provided written informed consent after receiving a full explanation of study procedures, risks, and potential benefits, as approved by the Zhengzhou University Ethics Committee.

### HD-tDCS neuromodulation protocol
In this study, all the patients received HD-tDCS (Model 4 × 1-C2; Soterix Med ical Inc., New York, NY), with 2 mA for 20 min. The 4 × 1 ring configuration of the HD-tDCS used Ag/AgCl ring electrodes to deliver a direct current to the scalp[27]. HD-tDCS targeted the Pz and F3 regions. The anode was positioned at the Pz and F3 locations in accordance with the international 10/20 system, and four cathodal electrodes were symmetrically arranged around the Pz or F3 areas, approximately 3.5 cm from the center (Fig. 2). We visualized a 3D rendering of the voltage and electric field distribution on an MNI152 averaged head using ROAST toolbox[28]. The sham
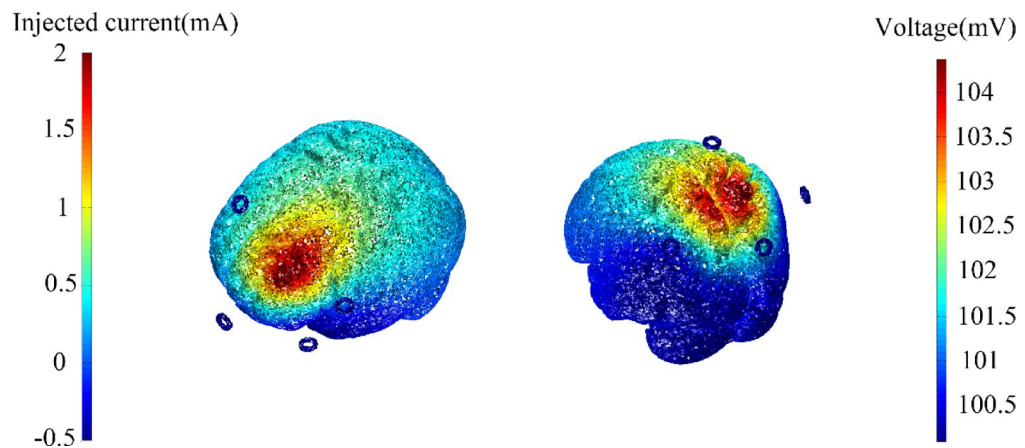
**Fig. 2**. The model of transcranial electric stimulation. Here we chose F3 and Pz as target, displaying 3D rendering of the computed voltage and electric field distribution.

condition had the same duration, electrode size and placement as the active condition. The ramp up/down was 15 and 30 s of stimulation was delivered at the beginning of the 20 min session to simulate the initial sensation of the active current. Patients underwent two daily neuromodulation sessions, one in the morning and one in the afternoon, over a period of 14 consecutive days. The sham group does not receive stimulation. Electroencephalographic (EEG) recordings were obtained prior to the commencement of tDCS and following the 14-day treatment period to monitor for any adverse effects associated with HD-tDCS[29].

## Clinical assessment protocol

The primary research objective focused on assessing the impact of HD-tDCS on patients' level of consciousness relative to the baseline CRS-R index and on identifying subsequent alterations in electrophysiological markers. We quantified changes in the CRS-R index pre- and post-stimulation across the three patient groups. Additionally, we meticulously monitored and documented any adverse events occurring during the stimulation sessions. The CRS-R Index, derived from the CRS-R, is a novel method specifically developed for the diagnosis of DoC. The CRS-R Index streamlines the scoring process by considering the highest scores across each subscale of the CRS-R, with the assumption that all lower-level items are also capable of scoring points. This index ranges from 0 to 100, and a cutoff value of 8.315 effectively differentiates patients in the unresponsive wakefulness syndrome (UWS) from those in the minimally conscious state (MCS). A key advantage of the CRS-R Index is its rapid and convenient calculation method, which aligns with the CRS-R scoring guidelines and facilitates the quantification of consciousness changes over time in DoC. Additionally, its computation does not necessitate the assessment of all CRS-R items, thereby minimizing patient fatigue and preventing the application of repeated painful stimuli[30].

## EEG recording and data preprocessing

The EEG equipment employed was a 20-channel Nicolet EEG amplifier from Natus Neurology Inc., featuring a digital sampling rate of 2500 Hz. Electrode placement conformed to the 10–20 system guidelines. Electrode-skin impedance was maintained below 5 kΩ throughout a 20-minute recording period. In certain cases, the CRS-R arousal stimulation protocol was administered immediately prior to EEG recording, ensuring that patients remained awake during data acquisition. EEG data from six patients were excluded due to suboptimal quality.

Consistent with our prior research, offline preprocessing was conducted using EEGLAB within the Matlab environment, supplemented by custom open-source scripts[31]. The EEG data underwent band-pass filtering within the 0.5–40 Hz range and notch filtering between 48 and 52 Hz. Subsequently, the data were downsampled to 250 Hz, re-referenced to the average, and segmented into non-overlapping intervals of 5 s each. The subsequent phase entailed the manual identification and excision of aberrant segments and channels, followed by interpolation for deficient channels. The final preprocessing step was the execution of independent component analysis on the EEG data to eliminate artifacts, including ocular and cardiac activities. Segments retaining less than 80% of data were deemed invalid[29].

## Resting-state EEG data analysis

In the analysis of resting-state EEG for patients with DoC, microstates and STE were employed to quantify the spatiotemporal dynamics and the directed information flow among brain regions. The EEG sequence was bandpassed into five frequency bands: delta (0.5–4 Hz), theta (4–8 Hz), alpha (8–13 Hz), beta (13–30 Hz), and gamma (30–40 Hz).

### Microstate analysis

The EEG time series was subjected to band-pass filtering within the 1–30 Hz frequency range. A peak detection algorithm identified local maxima in the Global Field Power (GFP), referred to as GFP peaks. For this research, 5000 GFP peaks were randomly selected and concatenated from each participant, yielding a total of 230,000 GFP peaks extracted pre-stimulation from the patients. The k-means algorithm within the + microstate toolbox

clustered the topographic maps, and the elbow method determined the optimal number of microstate clusters (k). Having identified the microstate maps, microstate labels were then assigned to each sample point for each patient to facilitate backfitting. Each GFP peak in the complete dataset was categorized with a specific microstate based on the closest microstate centroid map[23,32].

Global statistics for microstates included the Global Explained Variance (GEV) and the mean duration time. Specific statistics for microstate categories encompassed the mean duration of individual microstates, coverage (the proportion of time series represented by a microstate category), and occurrence (the frequency of a microstate's appearance per second)[33].

*Symbolic transfer entropy analysis*
We employed STE to quantify the flow of information, with THE combination of Transcranial Magnetic Stimulation and EEG (TMS-EEG) confirming its efficacy as an indicator of directed functional connections. We utilized the EEGapp pipeline (https://github.com/BIAPT/EEGapp) to compute STE values between each pair of the 20 electrodes[34,35]. We then compared the alterations in directed functional connectivity within the brain network pre- and post-stimulation across the three groups.

## Statistical analyses
Statistical analyses of behavioral data, microstate indices, and STE were conducted using the R statistical software (Version 4.2.1 R Core Team, 2022). We employed the Shapiro-Wilk test to assess the distribution characteristics of the data. Differences among the three groups were examined using the Mann-Whitney U test, while post-hoc analyses were performed with the Wilcoxon rank-sum test. The Signrank test was utilized to evaluate changes pre- and post-stimulation. To address multiple comparison concerns, we applied the False Discovery Rate (FDR) correction.

## Results
### Epidemiology characters
Between September 2020 and October 2023, of the 52 eligible patients with Disorders of Consciousness (DOC), 46 were included in the study (F3 group, $n=11$; Pz group, $n=16$; sham group, $n=19$). Exclusions comprised six patients due to persistent high impedance ($>5\,k\Omega$) despite repeated electrode adjustments, and EEG signal artifacts. Gender distribution included 5, 8, and 3 female patients in the F3, Pz, and sham groups, respectively, with no significant difference ($p=0.241$). The mean ages for the three groups were $55.9\pm19.5$, $56.3\pm7.18$, and $50.3\pm14.8$ years, respectively ($p=0.391$). Regarding etiology, the F3 group had 0, 8, and 3 instances of hypoxia, stroke, and brain trauma, respectively; the Pz group had 2, 11, and 3; and the sham group had 0, 14, and 5 ($p=0.583$). The CRS-R index prior to stimulation for the three groups were $17.6\pm19.7$, $12.9\pm12.3$, and $19.2\pm17.5$ ($p=0.520$), respectively. No significant differences were observed in clinical baseline characteristics among the groups, as shown in Table 1.

### Behavioral response characteristics after neuromodulation
Fourteen days after HD-tDCS stimulation, there were differences in the changes of CRS-R index among the three groups ($p=0.0228$), with post-hoc tests indicating that both F3 target ($p=0.0371$) and Pz target ($p=0.0117$) stimulation changes were higher than those of the sham group (Fig. 3A).

### Microstate indices
In this study, we analyzed resting-state EEG time series microstates in 46 patients. Sampling 210,000 GFP peaks before stimulation, we applied the k-means clustering algorithm to classify microstates for all subjects. Figure 4B depicts the variation in GEV with the number of states $k$ ranging from 2 to 20. The elbow method
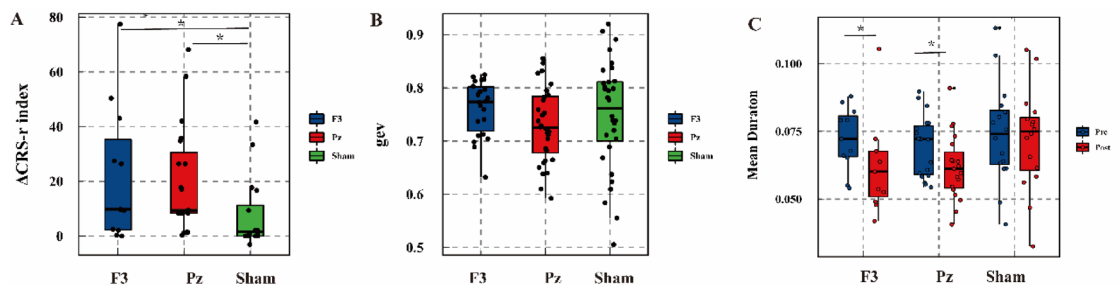


**Fig. 3.** CRS-r index change, CEV and mean duration of microstate before and after stimulation (F3 Pz and Sham). (**A**) F3 group has significantly increased CRS-r index ($p=0.0371$ FDR-corrected) compared to Sham group. Pz group has significantly increased CRS-r index ($p=0.0117$ FDR-corrected) compared to Sham group. (**B**) No significant difference was observed between the three groups in GEV. (**C**) After stimulation, the mean duration of microstate in the F3 and Pz groups exhibits a significant decrease($P=0.027$ and $p=0.021$ FDR_corrected).
*$p<0.05$ FDR-corrected, **$p<0.01$ FDR-corrected.

revealed that the optimal number of clusters for microstates is seven. For these states, the F3 group had a GEV of 76.7 ± 4.53%, the Pz group 72.8 ± 6.82%, and the sham group 75.0 ± 10.21%, with no significant differences between groups post hoc (see Fig. 3B). Figure 4A shows the spatial topography of the seven distinct microstates, labeled MS1 through MS7. Subsequently, we compared these microstates' attributes across groups. Both the F3 and Pz stimulation groups showed a decrease in average microstate duration after stimulation ($P = 0.027$ FDR_corrected and $P = 0.021$ FDR_corrected, respectively), as illustrated in Fig. 3C. Additionally, we performed a statistical analysis on the duration changes of each microstate pre- and post-neuromodulation within the F3 and Pz groups.

In the F3 group, the mean duration of microstates MS1 ($p = 0.0282$ FDR-corrected), MS2 ($p = 0.0313$ FDR-corrected), MS3 ($p = 0.0120$ FDR-corrected), MS4 ($p = 0.0294$ FDR-corrected), MS5 ($p = 0.0282$ FDR-corrected), MS6 ($p = 0.0120$ FDR-corrected), and MS7 ($p = 0.0337$ FDR-corrected) was shorter than before stimulation. Similarly, in the Pz group, the mean duration of microstates MS1 ($p = 0.0455$ FDR-corrected), MS2 ($p = 0.0415$ FDR-corrected), MS3 ($p = 0.0349$ FDR-corrected), MS4 ($p = 0.0415$ FDR-corrected), MS5 ($p = 0.0415$ FDR-corrected), MS6 ($p = 0.0249$ FDR-corrected), and MS7 ($p = 0.0293$ FDR-corrected) was also reduced post-stimulation compared to pre-stimulation conditions. The sham group showed no differences in the average duration of any microstates before and after stimulation.

Furthermore, the F3 group exhibited an increased occurrence rate of microstates MS4 ($p = 0.0449$ FDR-corrected) and MS5 ($p = 0.0449$ FDR-corrected) compared to pre-stimulation levels. The Pz group also demonstrated an elevated occurrence rate for microstates MS1 ($p = 0.0208$ FDR-corrected), MS2 ($p = 0.0208$ FDR-corrected), and MS7 ($p = 0.0492$ FDR-corrected) following stimulation. In contrast, the sham group did not exhibit any changes in the occurrence rates of the microstates before and after stimulation (Fig. 5).

## Symbolic transfer entropy

The Symbolic Transfer Entropy analysis was utilized to assess the directionality of information transfer within brain networks. In the theta band, the F3 group exhibited enhanced information flow from anterior to posterior regions, with a marked increase in intra-frontal communication during the alpha band. The study observed a strengthened bidirectional exchange of information between these brain regions. Enhanced inter-hemispheric connectivity in the beta band and augmented short-range information flow within frontal, parietal, and occipital regions in the gamma band were also noted. In contrast, the delta band presented a decline in information transfer from the left to the right hemisphere. Moreover, a diminished internal connectivity within the occipital lobes was observed in the beta and gamma bands.
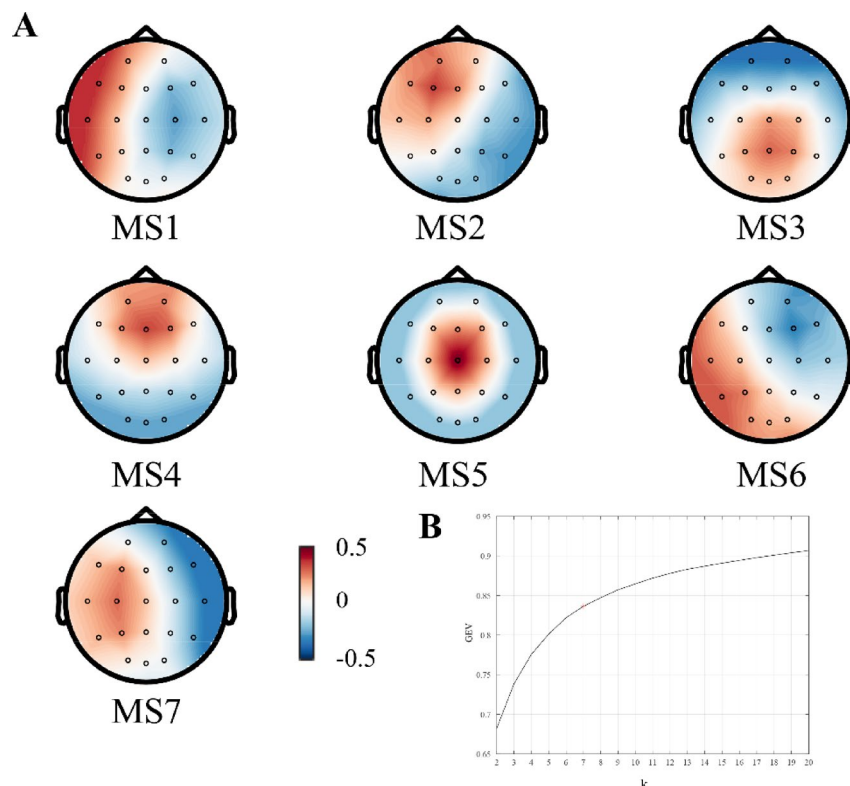


**Fig. 4**. Resting-state microstates. (**A**) GEV vs. number of states (k) for resting-state data. Here, GEV is calculated across the 230,000 peaks used for clustering. The kneedle algorithm found that k = 7 states was optimum, marked by a red "+." (**B**) Resting-state microstate maps derived from the k-means clustering algorithm for k = 7 states.
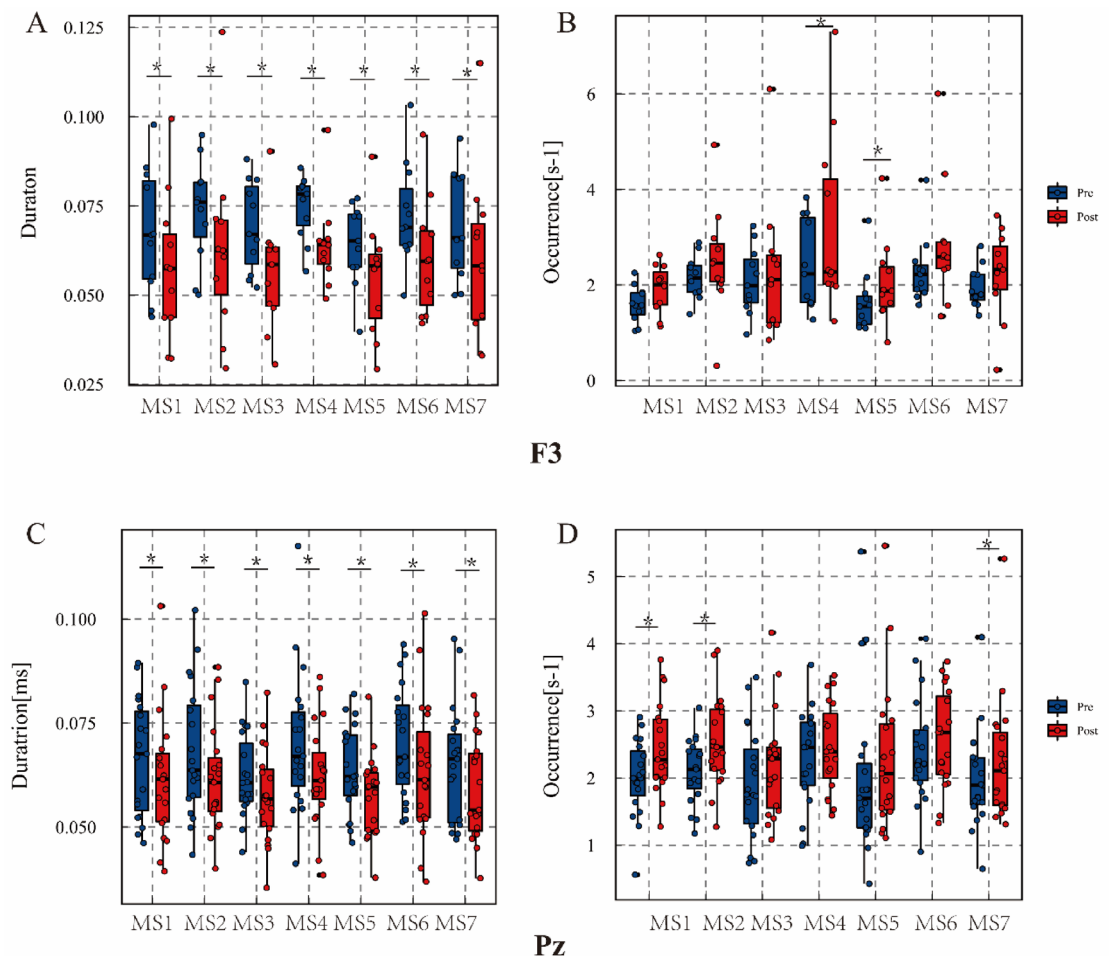
**Fig. 5**. Duration and occurrence of seven resting microstate maps before and after stimulation in the Fz3 and Pz groups. (**A**) The duration of all seven resting microstate maps decreased significantly after stimulation in the Fz group. (**B**) The F3 group showed a significant increase in the oooccurance of both microstates 4 and 5 after stimulation. (**C**) The duration of all seven resting microstate maps decreased significantly after stimulation in the Fz group. (**D**) The Pz group showed a significant increase in the oooccurance of microstates 1, 2 and 7 after stimulation. *$p < 0.05$ FDR-corrected, **$p < 0.01$ FDR-corrected.

The Pz group showed a predominant increase in information flow from the left frontal to parietal lobes within the theta and alpha bands, accompanied by a weakening of certain short-range connections within the frontal lobes in the delta, theta, and alpha bands. No significant changes in directed functional connectivity were observed in the sham group post-stimulation, as shown in Fig. 6.

## Discussion

In this research, we explored the impact of HD-tDCS on Pz and F3 targets in patients with DoC. Our results indicate notable alterations in EEG microstates and directed functional connectivity, hinting at a possible mechanism underlying the arousal effects induced by HD-tDCS. Both stimulation approaches have been found to enhance patient consciousness levels. Analysis of microstates and Symbolic Transfer Entropy reveals shared aspects in the neuromodulatory impact of varying targeted stimulation protocols; however, distinct differences also exist. These findings contribute to the ongoing debate regarding whether the genesis of consciousness is associated with anterior or posterior brain regions[36].

Our findings are consistent with prior research that emphasizes the significance of frontal and parietal regions in consciousness and cognitive function. Previous studies from our group have investigated the spatiotemporal dynamics of the brain and monitored EEG source-level microstate alterations during the natural recovery of consciousness in DoC patients, revealing distinct temporal dynamics, spatial activations, and associations with varying levels of consciousness[23]. In the current study, k-means clustering identified seven microstates in resting-state EEG data, delineating the activation patterns and spatiotemporal properties of the resting state. We analyzed the duration, coverage, and frequency of typical microstates, finding notable differences in the characteristics of instantaneous states due to the neuromodulatory effects of different stimulation targets. No significant differences in GEV were observed between groups, suggesting that microstates similarly encapsulate
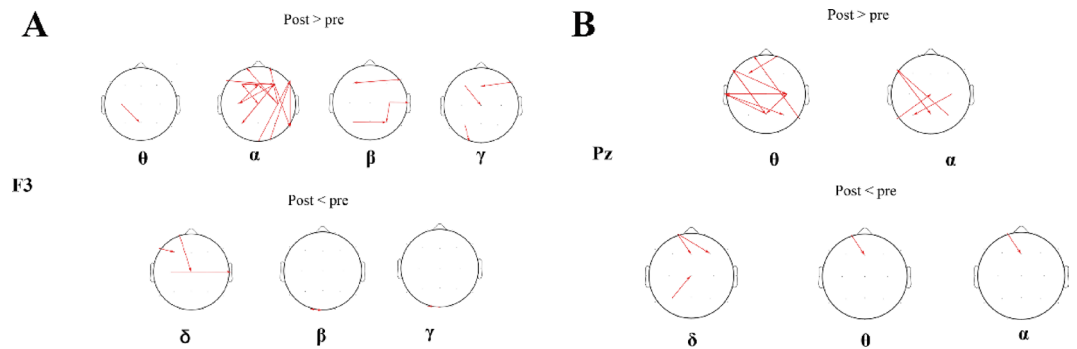
**Fig. 6**. Results of STE. (**A**) In group F3, edges with increased and decreased information flow in different frequency bands after stimulation (**B**) In group Pz, edges with increased and decreased information flow in different frequency bands after stimulation.

the EEG time series for all groups. Post-stimulation, both the F3 and Pz groups showed a reduction in mean duration time, indicating more efficient information transmission and processing within the same network patterns post-stimulation. Peng Gui et al. conducted a sensor-level microstate analysis of DoC patients, and the results were similar to those of this study, showing that the lower the level of consciousness, the longer the average time of microstates[37]. Our study corroborates that in consciousness research, extended microstate duration may reflect lower brain network dynamics, whereas shorter durations may facilitate quicker external information flow response and processing, potentially signifying higher consciousness levels. Custo et al. employed EEG to characterize spontaneous brain resting-state network (RSN) activations[38]. Through electric field topography analysis, seven resting-state topologies were inferred, matching broadband EEG scalp topographies to their source space-time patterns. The seven microstates identified in this study align with the topographic maps reported by Custo et al.: MS1 corresponds to the microstate G in this study, belonging to the sensorimotor network, with the main activation area in the cerebellum and central region; MS2 corresponds to the microstate B in this study, belonging to the visual and default mode network(DMN), with the main activation area in the occipital lobe. MS3 corresponds to the microstate C in this study, belonging to the default network, with the main activation area being the posterior cingulate cortex(PCC) and cuneus. MS4 corresponds to the microstate D in this study, belonging to the frontoparietal network (ECN), with the main activation area being the right superior and middle frontal gyrus and the right superior and inferior parietal lobule. MS5 corresponds to the microstate F in this study, belonging to the default network, with the main activation area being the medial prefrontal cortex. MS6 corresponds to the microstate A in this study, belonging to the default network and frontoparietal network (ECN), with the main activation area being the left temporal lobe and left insula. MS7 corresponds to the microstate E in the literature, belonging to the two key nodes of the default network before and after, with the main activation being the anterior cingulate cortex (ACC) and PCC[39].

The human resting-state brain network comprises multiple association areas within the cerebral cortex. The DMN facilitates intrinsic consciousness and self-referential processes via medial nodes in the medial prefrontal cortex, PCC, and precuneus. Additionally, the ECN located in the dorsolateral prefrontal cortex and posterior parietal cortex, mediates attention and environmental awareness. Preserving DMN functionality is beneficial for consciousness recovery following DoC. DMN activity correlates with patient consciousness levels and serves as a critical indicator for distinguishing between MCS and UWS[39].

In this study, the F3 group exhibited increased occurrences of MS4 and MS5, associated with the DMN and the anterior ECN, suggesting that F3-targeted stimulation primarily activates the anterior brain network. This activation enhances the anterior node of the DMN, the ACC, facilitating consciousness recovery. Furthermore, Symbolic Transfer Entropy analysis indicated that this stimulation protocol enhances bidirectional information flow within the anterior brain network in the alpha band and long-range connections between anterior and posterior regions. In the beta band, it promotes bidirectional communication across hemispheres, while in the higher gamma band, it increases short-range information flow within the anterior, posterior, and occipital lobes. In contrast, the lower delta band shows reduced information flow from the left to the right hemisphere, and the beta and gamma bands exhibit decreased occipital lobe connectivity. The arousal mechanism of the F3 stimulation protocol may involve activating the DMN, enhancing long-range connections in lower frequency bands, and strengthening short-range connections in higher frequency bands. The Pz group demonstrated increased occurrences of MS1, MS2, and MS7, encompassing the occipital lobe, ACC, PCC, and central region. These microstates include critical nodes of the DMN, visual network, and sensorimotor network. Compared to the F3 protocol, Pz stimulation also augments DMN activation, particularly its anterior and posterior key nodes. In the theta band, it increases internal and long-range anterior-posterior connections, while in the alpha band, it boosts inter-hemispheric and anterior-posterior connections, albeit weakening some short-range connections in lower frequency bands. These findings align with the theory that the brain typically exhibits increased long-range connections in lower frequencies and enhanced short-range connections in higher frequencies.

Bai et al. utilized single-pulse TMS-EEG to assess directed information flow in DoC patients. Their results indicated a loss of bidirectional flow in the frontal lobe, motor cortex, and parietal cortex. The interaction rate of TMS-induced networks between frontal and parietal cortices was significantly lower in UWS than in

MCS, correlating with clinical DoC scales, mirroring our findings[35]. Following both stimulation protocols, improvements in the CRS-R index were associated with increased bidirectional flow within the anterior brain network and enhanced frontal-parietal connectivity, indicating greater integration and stability.

The arousal mechanisms elicited by F3 and Pz stimulation protocols share certain features, yet exhibit distinct differences. Both protocols enhance activity within DMN, expedite information processing, and bolster the internal processing capacity of the anterior brain as well as the information transfer between anterior and posterior regions. The key distinction lies in the Pz protocol's ability to activate both anterior and posterior nodes of the DMN, whereas the F3 protocol predominantly influences the anterior node. At the same time, the main action frequency band of the F3 stimulation is higher, while the Pz stimulation is lower, respectively in the alpha and beta/theta and alpha band.

The structural organization of the human brain is optimized for information exchange to achieve more complex functions. The use of directed functional connectivity combined with the spatiotemporal dynamics represented by microstates has advanced our understanding of the brain's functional architecture and its relationship with human consciousness. Consistent with this study, the improvement of consciousness levels in patients with DOC is accompanied by the recovery of DOC network functions[40]. This study demonstrates that as consciousness levels increase, there is a significant increase in the inflow and outflow of information in the brain regions of DOC patients[35]. These findings are in line with the core proposition of the GWT, which suggests that the brain is divided into specialized modules that perform different functions, with long-distance connections between modules, such that the more information about a state is globally available, the more it can be consciously accessed. However, the GWT attributes consciousness to specific brain areas with an extensive broadcasting neuronal workspace (especially the frontal areas)[4]. Our study also found that the increased activation of the anterior and posterior nodes of the default network and the executive control network is accompanied by an enhancement of information flow within the anterior brain and between the anterior and posterior brains.

The recovery of effective information propagation (an increase in total information flow) directly reflects the recovery of causal interactions between brain regions. These findings are in line with the core tenets of IIT, which links consciousness to the causal structure of a system[41]. Information flow is essentially a frequency-specific measure of causal interactions, reflecting the intrinsic dynamics of corresponding cortico-thalamic circuits. Its recovery likely reflects changes in the thalamo-cortical and thalamo-occipital circuits in DOC patients after stimulation in the F3 and Pz groups. Previous research has shown that loss of consciousness is associated with the failure of two neural circuits: the inability of posterior cortical areas to convey information, combined with reduced information broadcasting in subcortical, temporal, parietal, and frontal areas. The mesoscale circuit model posits that thalamo-frontal and thalamo-parietal circuits are important pathways for the integration of consciousness-related information processing. Consistently, after the application of both stimulation protocols, there was an increase in activation of the anterior and posterior DMN network nodes, and an enhancement of connections between the anterior and posterior brain, with the F3 protocol showing a particularly increased activation of the executive control network. This supports the critical role of frontal and parietal areas in consciousness-related information flow, which is consistent with mainstream theories of consciousness[42]. In this study, both the F3 and Pz target stimulation protocols stimulate microstates related to the default network; the F3 mainly targets the anterior key node of the DMN, while the Pz stimulates both anterior and posterior nodes of the DMN. Both stimulation protocols also cause an increase in internal information flow within the anterior brain and information flow between the anterior and posterior brains. Although the arousal mechanisms of the two stimulation protocols are different, both highlight the interaction between the anterior and posterior brain as the cornerstone of consciousness generation[36].

## Limitations

Despite these promising results, our study has several limitations. The sample size was relatively small, limiting the generalizability of our findings. Furthermore, the quantity of EEG channels was limited, which may impact the robustness of our findings. While prior research has demonstrated that a minimum of 8 channels can reliably distinguish microstate patterns with high consistency, a minimum of 64 leads is necessary for accurate source reconstruction to determine the cortical origins of each microstate. Consequently, future research should employ high-density EEG for precise source localization. Moreover, our study was a prospective observational trial; hence, subsequent randomized controlled trials could yield more definitive interpretations of the data. Lastly, the segmentation of microstates might oversimplify the measurement of EEG dynamics. The "winner-takes-all" approach to labeling precludes the concurrent presence of competing microstate configurations during EEG segmentation and presupposes a discontinuous progression of EEG activity.

## Conclusion

In conclusion, our study underscores the potential of HD-tDCS)- in modulating brain activity to enhance arousal in patients with DoC. These findings enrich our comprehension of the neurophysiological underpinnings of consciousness and pave the way for novel therapeutic strategies. The study posits that consciousness emerges from the integrated functioning of the anterior and posterior brain regions. Moreover, it reveals an overlap in the mechanisms of action between the two stimulation protocols, proposing that a combined multi-target stimulation approach may offer a superior therapeutic modality.

## Data availability

## References

1. Seth, A. K. & Bayne, T. Theories of consciousness. *Nat. Rev. Neurosci.* **23**, 439–452. https://doi.org/10.1038/s41583-022-00587-4 (2022).
2. Brown, R. The HOROR theory of phenomenal consciousness. *Philos. Stud.* **172**, 1783–1794. https://doi.org/10.1007/s11098-014-0388-7 (2015).
3. Demertzi, A. et al. Human consciousness is supported by dynamic complex patterns of brain signal coordination. *Sci. Adv.* **5**, eaat7603. https://doi.org/10.1126/sciadv.aat7603 (2019).
4. Mashour, G. A., Roelfsema, P., Changeux, J. P. & Dehaene, S. Conscious processing and the global neuronal workspace hypothesis. *Neuron* **105**, 776–798. https://doi.org/10.1016/j.neuron.2020.01.026 (2020).
5. Marshall, W., Gomez-Ramirez, J. & Tononi, G. Integrated information and state differentiation. *Front. Psychol.* **7**, 926. https://doi.org/10.3389/fpsyg.2016.00926 (2016).
6. Tononi, G., Boly, M., Massimini, M. & Koch, C. Integrated information theory: From consciousness to its physical substrate. *Nat. Rev. Neurosci.* **17**, 450–461. https://doi.org/10.1038/nrn.2016.44 (2016).
7. Seth, A. K., Hohwy, J. & and Predictive processing as an empirical theory for consciousness science. *Cogn. Neurosci.* **12**, 89–90. https://doi.org/10.1080/17588928.2020.1838467 (2021).
8. Giacino, J. T., Fins, J. J., Laureys, S. & Schiff, N. D. Disorders of consciousness after acquired brain injury: The state of the science. *Nat. Reviews Neurol.* **10**, 99–114. https://doi.org/10.1038/nrneurol.2013.279 (2014).
9. Giacino, J. T., Kalmar, K. & Whyte, J. The JFK coma recovery Scale-Revised: Measurement characteristics and diagnostic utility. *Arch. Phys. Med. Rehabil.* **85**, 2020–2029. https://doi.org/10.1016/j.apmr.2004.02.033 (2004).
10. Di, H. et al. Chinese translation of the coma recovery scale-revised. *Brain Inj.* **31**, 363–365. https://doi.org/10.1080/02699052.2016.1255780 (2017).
11. Lefaucheur, J. P. et al. Evidence-based guidelines on the therapeutic use of transcranial direct current stimulation (tDCS). *Clin. Neurophysiol.: Official J. Int. Federation Clin. Neurophysiol.* **128**, 56–92. https://doi.org/10.1016/j.clinph.2016.10.087 (2017).
12. Thibaut, A., Schiff, N., Giacino, J., Laureys, S. & Gosseries, O. Therapeutic interventions in patients with prolonged disorders of consciousness. *Lancet Neurol.* **18**, 600–614. https://doi.org/10.1016/s1474-4422(19)30031-6 (2019).
13. Fan, W., Fan, Y., Liao, Z. & Yin, Y. Effect of transcranial direct current stimulation on patients with disorders of consciousness: A systematic review and meta-analysis. *Am. J. Phys. Med. Rehabil.* **102**, 1102–1110. https://doi.org/10.1097/phm.0000000000002290 (2023).
14. Mensen, A. et al. Decreased evoked slow-activity after tDCS in disorders of consciousness. *Front. Syst. Neurosci.* **14**, 62. https://doi.org/10.3389/fnsys.2020.00062 (2020).
15. Zhang, Y. et al. Neural correlates of different behavioral response to transcranial direct current stimulation between patients in the unresponsive wakefulness syndrome and minimally conscious state. *Neurol. Sci.: Off. J. Italian Neurol. Soc. Italian Soc. Clin. Neurophysiol.* **41**, 75–82. https://doi.org/10.1007/s10072-019-04034-8 (2020).
16. Wu, X. et al. Intrinsic functional connectivity patterns predict consciousness level and recovery outcome in acquired brain injury. *J. Neuroscience: Official J. Soc. Neurosci.* **35**, 12932–12946. https://doi.org/10.1523/jneurosci.0415-15.2015 (2015).
17. Wang, X. et al. Combined behavioral and mismatch negativity evidence for the effects of long-lasting high-definition tDCS in disorders of consciousness: A pilot study. *Front. NeuroSci.* **14**, 381. https://doi.org/10.3389/fnins.2020.00381 (2020).
18. Zhang, R. et al. Effects of high-definition transcranial direct-current stimulation on resting-state functional connectivity in patients with disorders of consciousness. *Front. Hum. Neurosci.* **14**, 560586. https://doi.org/10.3389/fnhum.2020.560586 (2020).
19. Cai, T., Xia, X., Zhang, H., Guo, Y. & Bai, Y. High-definition transcranial direct current stimulation modulates neural activities in patients with prolonged disorders of consciousness. *Brain Stimul.* **12**, 1619–1621. https://doi.org/10.1016/j.brs.2019.08.017 (2019).
20. S, A. A. et al. Analysis of EEG microstates as biomarkers in neuropsychological processes—review. *Comput. Biol. Med.* **173**, 108266, (2024). https://doi.org/10.1016/j.compbiomed.2024.108266
21. Manasova, D. et al. Dynamics of EEG microstates change across the spectrum of disorders of consciousness. *BioRxiv* https://doi.org/10.1101/2024.05.30.596582 (2024).
22. Michel, C. M. & Koenig, T. EEG microstates as a tool for studying the temporal dynamics of whole-brain neuronal networks: A review. *NeuroImage* **180**, 577–593. https://doi.org/10.1016/j.neuroimage.2017.11.062 (2018).
23. Zhang, C. et al. The temporal dynamics of large-scale brain network changes in disorders of consciousness: A microstate-based study. *CNS Neurosci. Ther.* **29**, 296–305. https://doi.org/10.1111/cns.14003 (2023).
24. Bai, Y. et al. Breakdown of effective information flow in disorders of consciousness: Insights from TMS-EEG. *Brain Stimul.* **17**, 533–542. https://doi.org/10.1016/j.brs.2024.04.011 (2024).
25. Ciprian, C., Masychev, K., Ravan, M., Reilly, J. P. & Maccrimmon, D. A. Machine learning approach using effective connectivity to predict response to clozapine treatment. *IEEE Trans. Neural Syst. Rehabil. Eng.: Publ. IEEE Eng. Med. Biol. Soc.* **28**, 2598–2607. https://doi.org/10.1109/tnsre.2020.3019685 (2020).
26. Staniek, M. & Lehnertz, K. Symbolic transfer entropy. *Phys. Rev. Lett.* **100** https://doi.org/10.1103/PhysRevLett.100.158101 (2008).
27. Kuo, H. I. et al. Comparing cortical plasticity induced by conventional and high-definition 4 × 1 Ring tDCS: A neurophysiological study. *Brain Stimul.* **6**, 644–648. https://doi.org/10.1016/j.brs.2012.09.010 (2013).
28. Huang, Y., Datta, A., Bikson, M. & Parra, L. C. Realistic volumetric-approach to simulate transcranial electric stimulation-ROAST-a fully automated open-source pipeline. *J. Neural Eng.* **16**, 056006. https://doi.org/10.1088/1741-2552/ab208d (2019).
29. Zhang, C. et al. Multidimensional assessment of electroencephalography in the neuromodulation of disorders of consciousness. *Front. NeuroSci.* **16** https://doi.org/10.3389/fnins.2022.903703 (2022).
30. Annen, J. et al. Diagnostic accuracy of the CRS-R index in patients with disorders of consciousness. *Brain Inj.* **33**, 1409–1412. https://doi.org/10.1080/02699052.2019.1644376 (2019).
31. Delorme, A. & Makeig, S. EEGLAB: An open source toolbox for analysis of single-trial EEG dynamics including independent component analysis. *J. Neurosci. Methods.* **134**, 9–21. https://doi.org/10.1016/j.jneumeth.2003.10.009 (2004).
32. Tait, L. & Zhang, J. +microstate: A MATLAB toolbox for brain microstate analysis in sensor and cortical EEG/MEG. *NeuroImage* **258**, 119346. https://doi.org/10.1016/j.neuroimage.2022.119346 (2022).
33. Tait, L. & Zhang, J. MEG cortical microstates: Spatiotemporal characteristics, dynamic functional connectivity and stimulus-evoked responses. *NeuroImage* **251**, 119006. https://doi.org/10.1016/j.neuroimage.2022.119006 (2022).
34. Zubler, F. et al. Stroke causes a transient imbalance of interhemispheric information flow in EEG during non-REM sleep. *Clin. Neurophysiol.: Off. J. Int. Federation Clin. Neurophysiol.* **129**, 1418–1426. https://doi.org/10.1016/j.clinph.2018.03.038 (2018).
35. Bai, Y. et al. Breakdown of oscillatory effective networks in disorders of consciousness. *CNS Neurosci. Ther.* **30**, e14469. https://doi.org/10.1111/cns.14469 (2024).
36. Boly, M. et al. Are the neural correlates of consciousness in the front or in the back of the cerebral cortex? Clinical and neuroimaging evidence. *J. Neurosci.: Off. J. Soc. Neurosci.* **37**, 9603–9613. https://doi.org/10.1523/jneurosci.3218-16.2017 (2017).
37. Gui, P. et al. Assessing the depth of Language processing in patients with disorders of consciousness. *Nat. Neurosci.* **23**, 761–770. https://doi.org/10.1038/s41593-020-0639-1 (2020).

38. Custo, A. et al. Electroencephalographic resting-state networks: Source localization of microstates. *Brain Connect.* **7**, 671–682. https://doi.org/10.1089/brain.2016.0476 (2017).
39. Yeo, B. T. et al. The organization of the human cerebral cortex estimated by intrinsic functional connectivity. *J. Neurophysiol.* **106**, 1125–1165. https://doi.org/10.1152/jn.00338.2011 (2011).
40. Edlow, B. L., Claassen, J., Schiff, N. D. & Greer, D. M. Recovery from disorders of consciousness: Mechanisms, prognosis and emerging therapies. *Nat. Reviews Neurol.* **17**, 135–156. https://doi.org/10.1038/s41582-020-00428-x (2021).
41. Ye, S., Kitajo, K. & Kitano, K. Information-theoretic approach to detect directional information flow in EEG signals induced by TMS. *Neurosci. Res.* **156**, 197–205. https://doi.org/10.1016/j.neures.2019.09.003 (2020).
42. Schiff, N. D. Recovery of consciousness after brain injury: A mesocircuit hypothesis. *Trends Neurosci.* **33**, 1–9. https://doi.org/10.1016/j.tins.2009.11.002 (2010).

## Acknowledgements

## Author contributions

Y.G.：developing algorithm and writing the manuscript. Y.Z. and L.W.：Data collection, Formal analysis. S.H. and D.A.：Data collection, Visualization. X.J., Z.P. and K.Z.：data collection and Data curation. Y.W.：conceived the study, interpretation of the results, and critical revision of the manuscript. C.Z.：conceived the study and was responsible for scientific integrity, data analysis, and writing the manuscript.

## Funding

## Declarations

### Competing interests

The authors declare no competing interests.

### Ethical approval and consent to participate

The Fifth Affiliated Hospital of Zhengzhou University's Ethics Committee sanctioned the study protocol, and consent was procured from the patients' next of kin and caregivers.

### Consent for publication

All authors agree to publish the article.

### Additional information

**Correspondence** and requests for materials should be addressed to Y.W. or C.Z.

**Reprints and permissions information** is available at www.nature.com/reprints.

**Publisher's note** Springer Nature remains neutral with regard to jurisdictional claims in published maps and institutional affiliations.